https://doi.org/10.5194/tc-2019-139
Preprint. Discussion started: 18 June 2019

The Cryosphere Discussions
Open Access
EGU

Investigating spatiotemporal patterns of snowline altitude at the end of melting season in High Mountain Asia, using cloud-free MODIS snow cover product, 2001-2016

Zhiguang Tang [1,*], Xiaoru Wang [1], Jian Wang [2], Xin Wang [1], Junfeng Wei [1]

[1] National-Local Joint Engineering Laboratory of Geo-spatial Information Technology, Hunan University of Science and Technology, Xiangtan 411201, China

[2] Key Laboratory of Remote Sensing of Gansu Province, Northwest Institute of Eco-Environment and Resources, Chinese Academy of Sciences, Lanzhou 730000, China

*****Correspondence to*: Zhiguang Tang (tangzhg11@hnust.edu.cn)

Abstract: The snowline altitude at the end of melting season (SLA-EMS) can be used as an indicator of the equilibrium line altitude (ELA) and therefore for the annual mass balance of glaciers in certain conditions. High Mountain Asia (HMA) hosts the largest glacier and perennial snow cover concentration outside the polar regions, but the spatiotemporal pattern of SLA-EMS under climate change is poorly understood in there. Here, we develop a method for estimating SLA-EMS over large-scale area by using the cloud-removed MODIS fractional snow cover data, and investigate the spatiotemporal characteristics and trends of SLA-EMS during 2001-2016 over the HMA. The possible linkage between the SLA-EMS and temperature and precipitation changes over the HMA is also investigated. The results are as follows: (1) There are good linear regression relationships (R = -0.66) between the extracted grid (30km) SLA-EMS and glaciers annual mass balance over the HMA. (2) Generally, the SLA-EMS in the HMA decreases with increase of latitude. And due to the mass elevation effect, it decreases from the high altitude region of Himalayas and inner Tibet to surrounding low mountainous area. (3) The SLA-EMS of HMA generally shows a rising trend in the recent years (2001-2016). In total, 75.3% (24.2% with a significant increase) and 16.1% (less than 1% with a significant decrease) of the study area show increasing and decreasing trends in SLA-EMS, respectively. The SLA-EMS significant increases in Tien Shan, Inner Tibet, south and east Tibet, east Himalaya and Hengduan Shan. (4) Temperature (especially the summer temperature) trends to be the dominant climatic factor affecting the variations of SLA-EMS over the HMA. Under the background of the generally losing glaciers mass in HMA, if the SLA-EMS continues to rise as a result of global warming, it will accelerate the negative mass balances of the glaciers. This study is an important step towards reconstruction the time series of glacier annual mass balance using SLA-EMS datasets at the scale of HMA to better document the relationships between climate and glaciers.

Keywords: snowline altitude; spatiotemporal patterns; High Mountain Asia; MODIS

1. Introduction

Snow and glaciers play an important role in the global energy and water cycles because of their high albedo and water storage properties, and can indicate the changes in global climate. Studying the variations of glaciers and

https://doi.org/10.5194/tc-2019-139
Preprint. Discussion started: 18 June 2019

snow is of significant importance in monitoring and maintaining water management for ecosystem processes and irrigation practices, because of there are more than one sixth of the global population relies on water from mountainous melt water (Barnett et al., 2005).

Snowline altitude and its inter- and intra-annual variability are key characteristics indicating temporal changes in snow cover and duration of snow melt (Krajčí et al., 2014). The concept of snowline estimation varies with the applications. In hydrological applications, the snowline is identified as the boundary separating snow-covered areas from snow-free areas (Kaur et al., 2010; Parker, 1997; Seidel et al., 1997), for estimation of snow covered area and its temporal evolution, which is hence used as an input for hydrological modeling (Holzer et al., 1995; Martinec et al., 2008), or for validation of snow model simulations (Turpin et al., 1997; Zappa, 2008). And, the snowline altitude estimates have also been applied as an alternative method for cloud removal in satellite snow cover products (Gafurov and Bárdossy, 2009; Parajka et al., 2010). In glacier and climate studies, the snowline defines the lowest altitude of the perennial snow cover (Flint, 1971), equivalent to the lower boundary of the snow covered area at the end of melting season (also known as snowline at end of melting season (Pandey et al., 2013)). The snowline altitude at the end of melting season (SLA-EMS) approximates the equilibrium line altitude (ELA), it can serves as a good proxy for ELA and therefore for the mass balance of glaciers (McFadden et al., 2011; Pandey et al., 2013; Rabatel et al., 2005, 2012; Tawde et al., 2016). Numerous studies (Braithwaite, 1984; Rabatel et al., 2005, 2008, 2012; WGMS, 1991-2013; Xie et al., 1996) have shown that glacier annual mass balance is highly correlated with the ELA and SLA-EMS, and it enables reconstruction of annual mass balance time series. The climate sensitivity of SLA-EMS has been generally emphasized as a supplement to current climate change indicator systems. A study of the spatial-temporal variations of the SLA-EMS can help in assessing the hydrologic cycle balance as well as to understand the regional and global cryosphere and climate changes.

High Mountain Asia (HMA) hosts the largest perennial snow and glacier concentration outside the Antarctic and Arctic regions. As one of the most sensitive and prominent areas responding to global climate changes, the temperature of the HMA has increased more than twice the rate of global warming in the past decades (Hu et al., 2013; Qiu, 2008); and the snow cover and glaciers in HMA are in a state of rapid change (Brun et al., 2017; Rittger et al., 2016; Yao et al., 2012). These have led to changes in mountainous hydrological processes and water resources, and increased the HMA's runoff due to the accelerated glacier/snowmelt (Chen et al., 2017; Duethmann et al., 2015; Lutz et al., 2014). Meltwater from snow and glaciers in HMA provides a major source of water for approximately 1.4 billion of inhabitants in the downstream low lying plains (Immerzeel et al., 2010). Changes in the SLA-EMS with the increase or reduction of perennial snow- and ice-covered area have a profound effect on stream water availability in the basins (Lei et al., 2012). For the future livelihood of these people, it is therefore very important to estimate the SLA-EMS in HMA, understand how the SLA-EMS will respond to climate changes.

The traditional strategy for SLA-EMS estimating is direct ground-based observations using field methods, and extrapolating them to the rest of the mountain ranges. In HMA, this strategy suffers from the scarcity of local observations in space and time and the consequent need to extrapolate to vast unsampled areas. This is problematic, given that the pattern of glacier change in HMA is now known to be strongly heterogeneous (Brun et al., 2017). Satellite remote sensing offers the opportunity to extract and evaluate snowline in the inaccessible areas with rugged terrain and hostile climate. Most previous studies (McFadden et al., 2011; Pandey et al., 2013; Rabatel et al., 2005, 2012; Tawde et al., 2016; Zhang and Kang, 2017) of SLA-EMS have focused on local areas

https://doi.org/10.5194/tc-2019-139
Preprint. Discussion started: 18 June 2019


The Cryosphere Discussions
Open Access
EGU

and using visual interpretation of Landsat MSS/TM /ETM+ and SPOT images observed in the end of summer in which the snow cover extent is at its minimum value. However, they are difficult to assess SLA-EMS changes in a continuous time and space for a large-scale area, due to the 16-day or longer revisit period and relatively small swath width of Landsat and SPOT.

The most recent and advanced remote sensing snow cover product is produced by MODIS flown on the Earth Observing System (EOS) Terra and Aqua platforms. The MODIS snow cover products (Riggs et al., 2006) have been widely used to depict the spatiotemporal patterns of the seasonal or transient snowline altitude in mountainous areas (Krajčí et al., 2014; Krajčí et al., 2016; Parajka et al., 2010; Spiess et al., 2016; Tang et al., 2014; Verbyla et al., 2017), although they were rarely used to evaluate the SLA-EMS. Evaluation studies have suggested a high accuracy of MODIS snow cover products under clear skies, when comparing with the in-situ observations and other higher resolution satellite data at both regional and global scales (Hall and Riggs, 2007; Klein et al., 2003; Tang et al., 2013). However, the extensive cloud obscuration in MODIS snow cover products greatly limits their applications (Hall and Riggs, 2007; Riggs et al., 2006). Due to the MODIS fractional snow cover (FSC) maps more accurately represent the gradual changes of snow cover in each pixel than the binary snow cover maps (Riggs et al., 2006; Salomonson and Appel, 2004), the use of the FSC data could be better for the removal of the cloud cover by temporal filtering. Consequently, we have developed a cubic spline interpolation cloud removal method to eliminate the cloud covered pixels from the MODIS FSC products (Tang et al., 2013), and the cloud removal method was well applied in Tibetan Plateau and Tianshan Mountains (Tang et al., 2013, 2014, 2017). The advantage of the cloud removed MODIS FSC products is that the FSC changing curve (the characteristic of gradual changes) for each pixel are considered rather than the simple substitution by multiday combination for the binary snow cover products (Wang and Xie, 2009; Xie et al., 2009; Zhang et al., 2016b), and all of the cloud pixels and other missing or abnormal pixels are removed with a high snow-classification accuracy, thus providing considerable application value for snow cover monitoring.

The objectives of this paper are to: (1) propose a method for estimation of SLA-EMS over a large-scale area, based on the cloud-removed daily MODIS FSC data; (2) give spatially detailed estimates of the changes of SLA-EMS in HMA during 2001-2016 on a grid-by-grid basis. We also examine the SLA-EMS changes from different subregions of the HMA, and the possible cause for the SLA-EMS changes from the perspective of climate factors (temperature and precipitation). The topic is important as it will help to improve our understanding of the climate-cryosphere relationship at the scale of a whole HMA. This study will also be an important step towards reconstruction the time series of glacier annual mass balance using SLA-EMS datasets at the scale of HMA to better document the relationships between climate and glaciers.

2. Study area and data

2.1. Study area

The HMA is the largest and highest mountain region on earth, stretching across Central Asia between 65°-105°E and 25°- 51°N (Figure 1). It covers an area over 5 million km2, with the average elevation over 4000 m, spanning regions from the Hindu Kush and Pamir in the west to the Hengduan Mountains in the east, from Himalayas in the south to the Altay and Sayan in the north. Based on mountain ranges, HMA was subdivided into 16 subregions (Figure 1).

https://doi.org/10.5194/tc-2019-139
Preprint. Discussion started: 18 June 2019

The Cryosphere
Discussions
Open Access
EGU

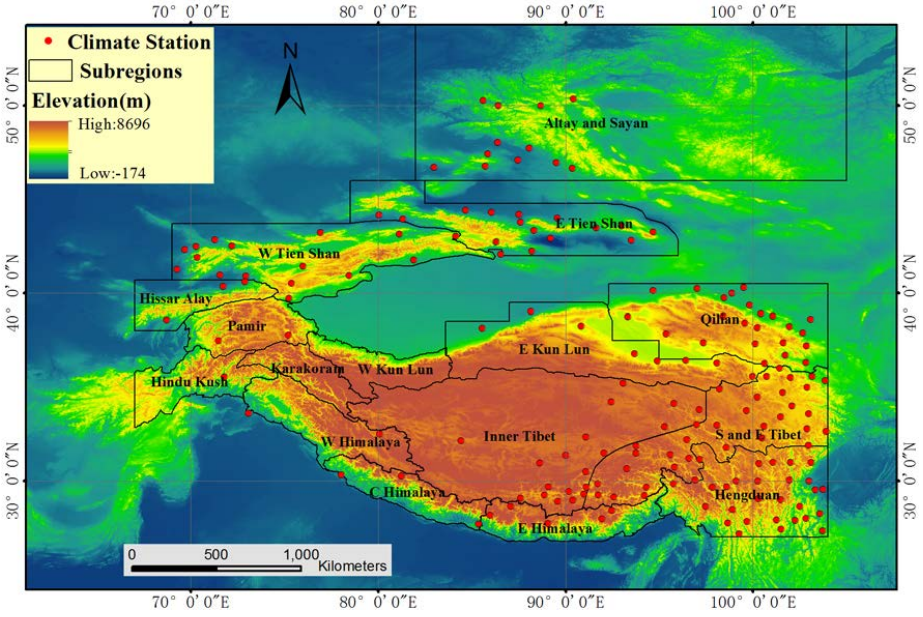

Figure 1. Location and the extent of the study area and subregions. Red dots denote meteorological stations. In names of subregions, these individual letters 'W', 'C', 'E' and 'S' mean west, central, east and south, respectively.

2.2. Data

2.2.1. MODIS Fractional Snow Cover (FSC) Data

In this study, the MOD10A1 data for 2001–2016 from the National Snow and Ice Data Center (NSIDC) (https://nsidc.org/) are employed to investigate the SLA-EMS variations in the HMA. MOD10A1 data are daily snow cover products, which include both binary snow cover and fractional snow cover (FSC) products (with a resolution of 463.3 m), gridded in sinusoidal projection (Riggs et al., 2006). The MODIS FSC mapping algorithm is developed by Salomonson and Appel (Salomonson and Appel, 2004), which is based on a statistical-linear relationship developed between the normalized-difference snow index (NDSI) from MODIS and the true subpixel fraction of snow cover as determined using Landsat scenes. Evaluation studies have proved a high accuracy (with a mean absolute error less than 0.1) of the MODIS FSC data (Hall and Riggs, 2007; Salomonson and Appel, 2004; Tang et al., 2013) . Using the MODIS Reprojection Tool (MRT) (Dwyer and Schmidt, 2006), the MOD10A1 FSC data are mosaicked and resampled from the original 463.3 m pixel size to 500 m, and georeferenced into a UTM projection with a datum of WGS84. The final mosaicked images are converted to GeoTIFF file format.

2.2.2. Meteorological Observation Data

Daily temperature and precipitation from 172 meteorological stations (Figure 1) in the HMA for 2001–2016 are collected from China Meteorological Administration (http://data.cma.cn) and NOAA's National Centers for Environmental Information (NCEI) (https://www.ncdc.noaa.gov/), formerly known as National Climatic Data

https://doi.org/10.5194/tc-2019-139
Preprint. Discussion started: 18 June 2019

Center. The temperature and precipitation data are used to survey the linkages between SLA-EMS changes and climate variations during the study periods.

2.2.3. Glacier Annual Mass Balance Observation Data

The Fluctuations of Glaciers Database (2017)((WGMS), 2017) (DOI: 10.5904/wgms-fog-2017-10) is collected from World Glacier Monitoring Service (WGMS, https://wgms.ch/data_databaseversions/). It is an internationally collected, standardized dataset on changes in glaciers (length, area, volume and mass), based on in-situ and remotely sensed observations, as well as on reconstructions. In this study, 12 observed glaciers (Figure 2) with the annual mass balance observations over 6 years (and 8 of them are observed over 10 years) are selected as calibration data for the SLA-EMS estimation.

2.2.4. Other Data

The digital elevation model (DEM) data at the spatial resolution of 90 m from the Shuttle Radar Topography Mission (SRTM) are used to derive the altitude values of SLA-EMS. They are available at http://srtm.csi.cgiar.org/. In order to match the MODIS images, the SRTM DEM are resampled from the original 90-m pixel size to 500 m. The glacier inventory data (Figure 2) used in this study includes the Second Glacier Inventory Dataset of China (http://westdc.westgis.ac.cn/data) and the Randolph Glacier Inventory 5.0 (RGI 5.0, http://www.glims.org/RGI/randolph50.html); the RGI 5.0 is used for the study areas of outside China. Besides, several Landsat TM/ETM+/OLI images of the five selected Landsat scenes (Figure 2) are also used as reference data for the SLA-EMS estimation.

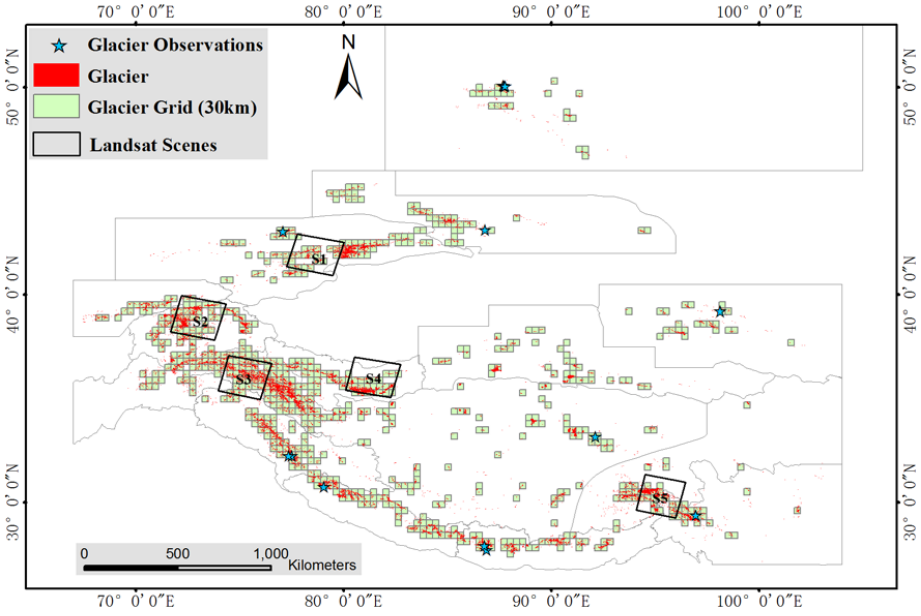

Figure 2. Spatial distribution of glacier grids, glacier observations and Landsat scenes. The annual mass balance observations of 12 observed glaciers (listed in Table 1) are collected from the Fluctuations of Glaciers Database (https://wgms.ch/data_databaseversions/). Glacial areas in the HMA are divided into 744 glacial

https://doi.org/10.5194/tc-2019-139
Preprint. Discussion started: 18 June 2019

grids with the cell size of 30km. The five black boxes (S1-S5) outline the area covered by Landsat images (in Table 2).

3. Methods

3.1. Cloud Removal from MODIS FSC Data, and SCD Calculation

Following the cloud removal method for MODIS FSC products developed by Tang et al. (Tang et al., 2013), the daily cloud-removed FSC data in the study area were produced from 2000 to 2016. The cloud removal algorithm is based on the cubic spline interpolation algorithm (temporal filtering). Details on the cubic spline interpolation cloud removal method and the relevant accuracy evaluation strategies can be found in the works of Tang et al. (Tang et al., 2013). From the applications of the cloud removal method in the areas of HMA (Tibetan Plateau and Tianshan Mountains) (Tang et al., 2014; Tang et al., 2013; Tang et al., 2017), the cloud removal method was efficient in retrieving the FSC information of these cloud covered pixels in these areas, with the overall mean absolute error less than 0.1; and there was a high consistency between MODIS-derived snow-covered days (SCD) and the in-situ observed SCD, the mean consistency over 85%, and the mean absolute error is less than 4.2 days (Tang et al., 2014; Tang et al., 2013; Tang et al., 2017). The higher consistency between MODIS-derived SCD and in-situ SCD indicates that the cloud-removed MODIS FSC data have a high accuracy to monitor the snowline in the HMA.

The SCD represents the overall snow cover conditions for a region in a year. Therefore, the maps of the spatial distribution of SCD have potential significance for SLA-EMS determination. In this study, the SCD images are calculated using all cloud-free MODIS FSC images for a given year. The calculation equation is shown as:

$$SCD=\sum_{i=1}^{N} Ceil(D_i \geq 50) \quad (1)$$

where N is the total number of days (images) within a year and Di is the snow cover fraction (%) in a pixel($0 \leq Di \leq 100$). Ceil ($Di \geq 50$) counts the numbers of $Di \geq 50$. For instance, if the pixel value on the image is 60 (i.e., 60% snow cover), the SCD adds 1. If the pixel value on the image is 10 (i.e., 10% snow cover), the SCD adds 0 and is unchanged. Figure 3 shows the distribution of the MODIS-derived SCD in the HMA.

https://doi.org/10.5194/tc-2019-139
Preprint. Discussion started: 18 June 2019

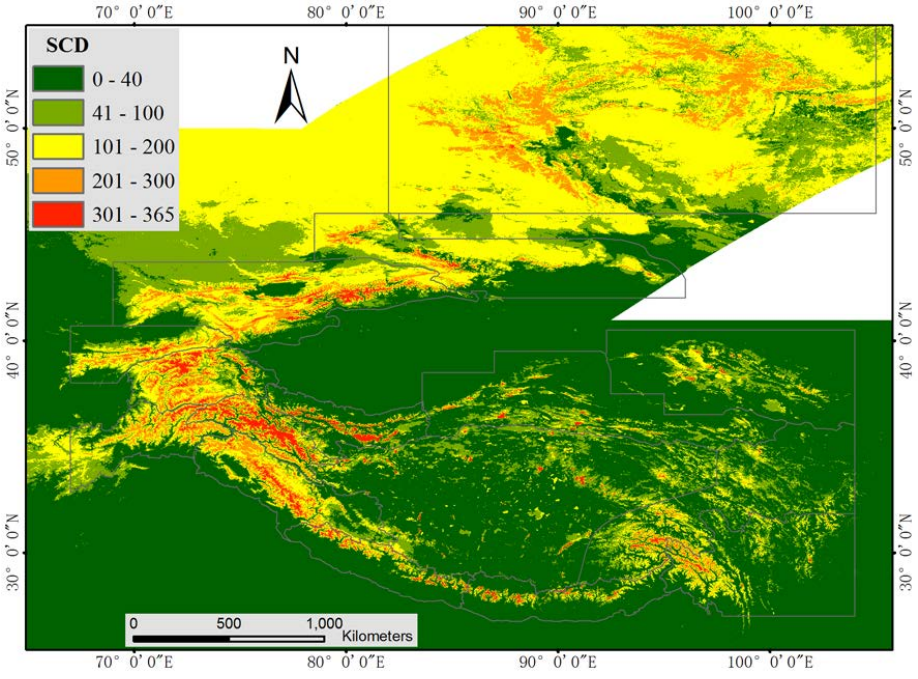

Figure 3. Distribution of average snow-covered days (SCD) from 2001 to 2016 in the High Mountain Asia (HMA).

3.2. Methodology of SLA-EMS monitoring

For snow cover, the end time of melting season varies with the places and years, so that perennial snow cover (i.e., the snow cover at the end of melting season) in a range of HMA is difficult to identify in terms of the snow cover on a specific given date. Theoretically, the SLA-EMS can be determined by the MODIS derived snow covered days (SCD), that is, the boundary altitude of perennial snow cover (where the SCD≥365d). However, the snow area with MODIS SCD≥365d is fail to really indicates the perennial snow area, due to the affection of the annual cumulated errors in MODIS snow mapping algorithm and cloud removal method. For instance, our previous studies (Tang et al., 2013; Tang et al., 2017) in Tibetan plateau and Tianshan Mountains have found that the snow areas with MODIS SCD≥365d are far less than the glacier areas, although the clouds in MODIS snow product are effectively eliminated. In addition, how to estimate the boundary altitude value of the perennial snow cover is another problem need to be solved. Therefore, the designed methods of monitoring the SLA-EMS from cloud-removed MODIS FSC products in this study involve (1) dividing glacier grids, (2) calibration of MODIS SCD threshold for perennial snow cover estimation, (3) determination the boundary altitude value of the perennial snow cover.

3.2.1. Dividing Glacier Grids

In order to make detailed and comprehensive assessments of the SLA-EMS, glacial areas in the HMA are divided into 744 grids (named glacier grids) with the cell size of 30km (Figure 2). For each identified glacier grid, the area of glacier cover is ensured to be more than 25km2 based on overlay analysis with the glacier

https://doi.org/10.5194/tc-2019-139
Preprint. Discussion started: 18 June 2019

inventory data. Thus, the SLA-EMS in the HMA can be investigated thoroughly on a grid-by-grid and year-by-year basis.

3.2.2. Calibration of MODIS SCD Threshold for Estimating Perennial Snow Cover

Since SLA-EMS is able to serves as a good proxy for ELA and thus for the mass balance of glaciers, it is reasonable to calibration of MODIS SCD threshold value by comparing the correlations between the SLA-EMS and annual mass balance of glaciers. In this method, the annual mass balance observations of the 12 measured glaciers (Figure 2) are used as reference data for SCD threshold calibration, and yearly SLA-EMS values of the corresponding glacier grids are extracted for any given SCD values (setting the SCD threshold changing from 280 to 365d, with 1d as the step size). Here, the method of SLA-EMS values extraction is shown in section 3.2.3. Figure 4 shows the average correlation coefficients between annual mass balance of the 12 glaciers and the SLA-EMS changing with the MODIS SCD threshold. As the MODIS SCD growing, the negative correlations enhanced, and peaked when SCD is 347d, and then decreased rapidly, indicating that 347d is an optimal SCD threshold (Figure 4). With SCD changing from 348 to 365d, the rapid decreasing of the negative correlations could be attributed to annual cumulated errors in MODIS snow mapping algorithm and cloud removal method, thus the high SCD (from 348 to 365d) is not suit for the threshold to estimating perennial snow cover and SLA-EMS. Using MODIS SCD threshold as 347d, the scatter plots and linear regression parameters between glacier annual mass balances and grid SLA-EMS (30km) for the 12 measured glaciers are shown in Figure 5 and Table 1. They show that the 30km SLA-EMS extracted with 347d as MODIS SCD threshold has significant linear relation with glacier annual mass balance.

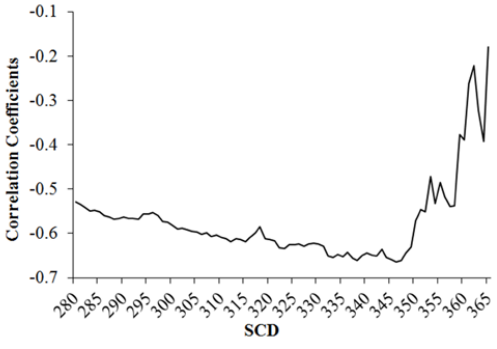

Figure 4. Average correlation coefficients between annual mass balance of the 12 measured glaciers and their corresponding grid (30km) snowline altitude at the end of melting season (SLA-EMS), changing with the MODIS snow covered-days (SCD) threshold. The peaked negative correlations when SCD is 347d, indicating that 347d is an optimal MODIS SCD threshold for extraction of SLA-EMS.

https://doi.org/10.5194/tc-2019-139
Preprint. Discussion started: 18 June 2019

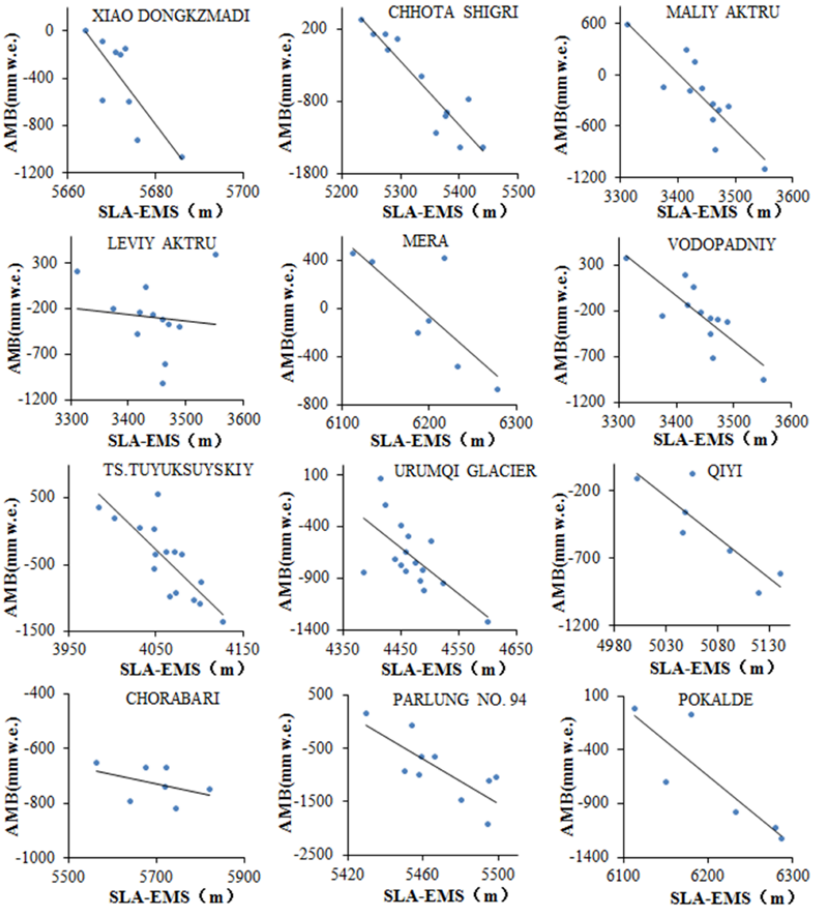

Figure 5. Scatter plots between glacier annual mass balances (AMB) and their corresponding grid (30km) snowline altitude at the end of melting season (SLA-EMS) for the 12 measured glaciers. The MODIS SCD threshold of 347d is used in the extraction of SLA-EMS.

Table 1. Linear regression parameters between annual mass balances (y) and the extracted 30km grid SLA-EMS (x) for the 12 measured glaciers.

Glaciers	Number of observations (yr)	Linear fitting equation	Correlation coefficients (R)
XIAO DONGKZMADI	10	y = -49.359x + 279566	-0.8
CHHOTA SHIGRI	12	y = -8.8258x + 46542	-0.93
MALIY AKTRU	12	y = -6.7223x + 22876	-0.85
LEVIY AKTRU	12	y = -0.7471x + 2283.9	-0.11
MERA	8	y = -6.4232x + 39766	-0.76
VODOPADNIY (NO.125)	12	y = -5.0136x + 17001	-0.82
TS.TUYUKSUYSKIY	16	y = -12.608x + 50791	-0.76
URUMQI GLACIER NO. 1	16	y = -4.4547x + 19215	-0.65

https://doi.org/10.5194/tc-2019-139
Preprint. Discussion started: 18 June 2019

QIYI	7	y = -6.0463x + 30172	-0.71
CHORABARI	7	y = -0.3482x + 1257.1	-0.44
PARLUNG NO. 94	10	y = -20.797x + 112856	-0.6
POKALDE	6	y = -6.415x + 39131	-0.57

In addition, we also use several Landsat TM/ETM+/OLI images of 5 selected Landsat scenes to determine the MODIS SCD threshold for estimating perennial snow cover. In the process of Landsat images selection, we focus on the principle of that the imaging time is near the end of summer and are almost unaffected by the cloud. The specific dates and locations of Landsat ETM+/OLI images are listed in Figure 2 and Table 2. In this work, Landsat images are firstly classified as snow or non-snow using the current "SNOWMAP" (Hall et al., 1995) approach. And then the perennial snow cover maps (minimized snow cover) for each Landsat scenes are produced from a composite of multi-images, in which the pixel will be identified as perennial snow cover only if it is classified as snow in all the selected images of the scene. Finally, we compare the Landsat-derived perennial snow cover against that of MODIS-derived in the 5 Landsat scenes, and changing with the MODIS SCD threshold. As Figure 6 shows, although the optimal SCD thresholds (with the area ratio is equal to 1) are varying with the regions, the average of them is also about 347d. Therefore, in this study, we ultimately chose the MODIS SCD thresholds as 347d for estimating perennial snow cover and SLA-EMS.

Table 2. Information about Landsat images used in calibration of MODIS SCD threshold.

Region	Sensor	Date	Path	Row
S1	OLI	2013/07/30、2013/08/15、2013/08/31、2013/09/16	148	31
S2	OLI	2014/07/22、2014/08/07、2014/08/23、2014/09/08	151	33
S3	OLI	2013/07/08、2013/07/24、2013/08/25、2013/09/10	149	35
S4	TM	2009/06/28、2009/07/30、2009/08/15、2009/08/31	145	35
S5	ETM+	2002/07/13、2002/07/29、2002/08/14、2002/08/30	135	39

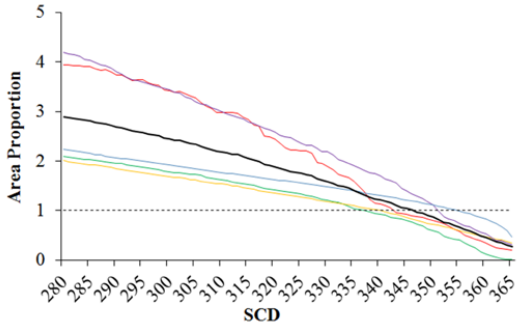

Figure 6. Comparisons of Landsat-derived perennial snow cover area and that of MODIS-derived in the 5 Landsat scenes (Region S1-S5 in Figure 2 and Table 2), changing with the MODIS SCD threshold. The Y-axis represents the area ratio of Landsat-derived perennial snow cover area divide by that of MODIS-derived, and bold black line represents the averages of the 5 regions.

https://doi.org/10.5194/tc-2019-139
Preprint. Discussion started: 18 June 2019

3.2.3. Determination Boundary Altitude Value of Perennial Snow Cover

Determination the altitude value of the SLA-EMS for every glacier grid (30km) is carried out using the area-elevation distribution curve and the perennial snow cover area. The area-elevation distribution curve for each glacier grid is generated using the resampled SRTM DEM data (500m). Take one of glacier grids as an example, the elevation measuring graph of the area-elevation distribution curve is shown in Figure 7. The altitude value of SLA-EMS for a particular year of a grid is calculated by selecting the elevation for which the area above this elevation is equal to the perennial snow cover area in the grid. Thus, the SLA-EMS in the HMA is able to be measured on a grid-by-grid basis, as long as the yearly perennial snow cover area was accurately obtained.

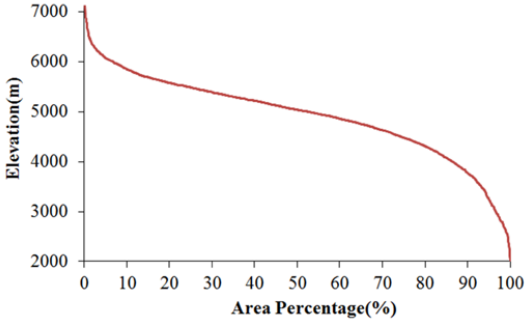

Figure 7. An example of area-elevation distribution curve for one of the glacier grids. The X-axis represents the percentage area above the corresponding elevations (Y-axis) in the grid.

3.3. Methodology of SLA-EMS Changes and the Linkages with Climate Factors

Trend analysis of a time series consists of the magnitude of trend and its statistical significance. Linear regression analysis is one of the most common methods of simulating the change trend of a time series. In this study, the ordinary least squares (OLS) regression is employed to calculate the linear trends of the SLA-EMS over the 16 years. A trend is considered to be statistically significant if its significance levels at 5%. Specifically, the slope of the least-squares line fitting of the SLA-EMS is calculated as:

$$Slope = \frac{n \times \sum_{i=1}^{n} i \times SLA_i - \sum_{i=1}^{n} i \sum_{i=1}^{n} SLA_i}{n \times \sum_{i=1}^{n} i^2 - \left(\sum_{i=1}^{n} i \right)^2} \quad (2)$$

where, Slope is the slope of the least-squares line fitting; i is the serial number from 1 to 16 for the years from 2001 to 2016; n is the cumulative number of years; and SLAi is the value of SLA-EMS in the ith year. When Slope > 0, there is an increasing tendency; when Slope = 0, there is no increasing or decreasing tendency; when Slope < 0, there is a decreasing tendency. And their significance levels (P) of F-test are presented.

Pearson correlation analysis is used to investigate the correlations between SLA-EMS, and temperature and precipitation dynamics for the 16 years (2001-2016). Pearson correlation coefficient (r) is a measure of the linear correlation between two variables x and y, which can be calculated with Equation (3)

https://doi.org/10.5194/tc-2019-139
Preprint. Discussion started: 18 June 2019

$$r_{xy} = \frac{\sum_{i=1}^{n}(x_i - \bar{x})(y_i - \bar{y})}{\sqrt{\sum_{i=1}^{n}(x_i - \bar{x})^2}\sqrt{\sum_{i=1}^{n}(y_i - \bar{y})^2}} \quad (3)$$

where r_{xy} is the correlation coefficients between x and y; x is the SLA-EMS, y is the temperature or precipitation; n is the number of the samples; $\bar{x}$ and $\bar{y}$ denote the average values of the x and y, respectively. Since the correlation coefficients are determined in the period from 2001 to 2016, n equals to 16 here. The correlation is considered to be significant if it is at the 5% significance levels.

4. Results

4.1 Spatial Pattern of SLA-EMS

For each glacier grid (30km) in the HMA, the yearly SLA-EMS has been calculated. Figure 8 presents the spatial patterns of SLA-EMS in the HMA during 2001-2016. The spatial changes of the SLA-EMS (from 3114 to 6907m) exhibit a large spatial heterogeneity in the HMA (Figure 8). The average SLA-EMS (6091 m) in east Himalaya is the highest among the different subregions, while the lowest (3575 m) is in Altay and Sayan. From the whole of the HMA, the average SLA-EMS is 5256 m (Figure 9).

Generally, the SLA-EMS in the HMA decreases with increase of latitude; in southern HMA (such as the east and central Himalayas, inner Tibet), the SLA-EMS in many grids higher than 6200m, while in northern HMA (the Altay and Sayan), they are less than 3200m (Figure 8). Furthermore, from the high altitude region of Himalayas and inner Tibet to surrounding low mountainous area, the SLA-EMS gradually decreases; and there is a significant positive correlation between SLA-EMS and elevation, which indicates the spatial patterns of the SLA-EMS are also controlled by the change of altitude (Figure 10).

https://doi.org/10.5194/tc-2019-139
Preprint. Discussion started: 18 June 2019

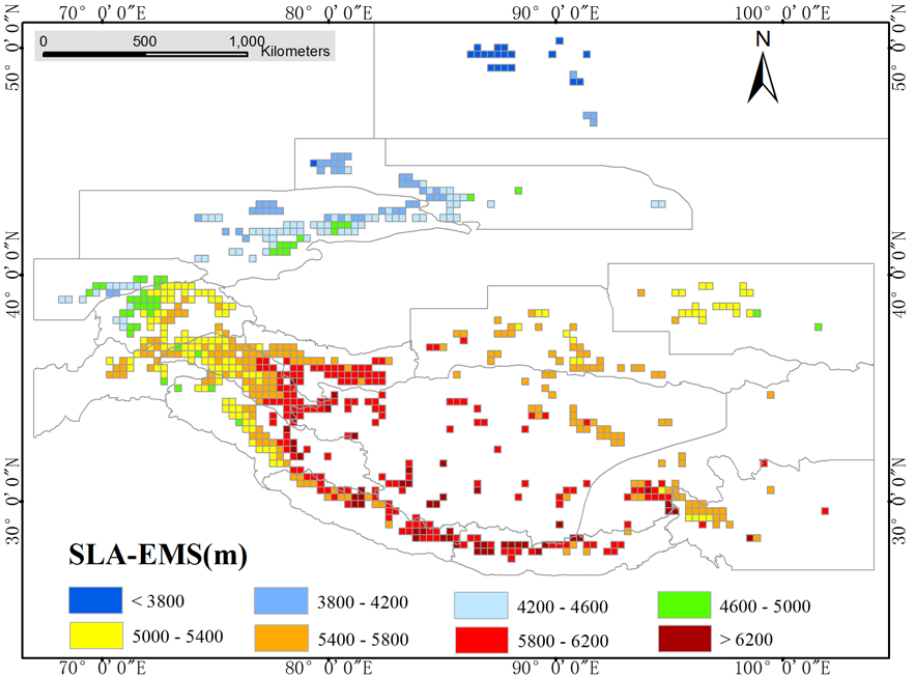

Figure 8. Spatial patterns of average SLA-EMS in the HMA for 2001-2016.

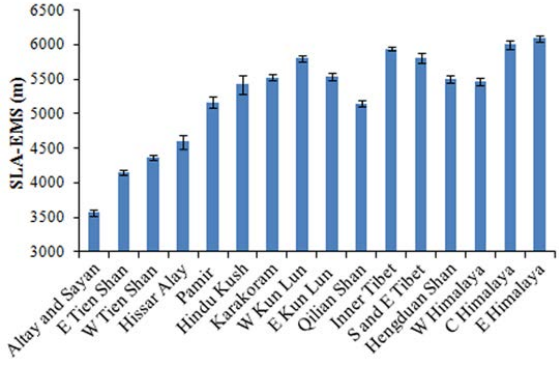

Figure 9. Average SLA-EMS for different subregions. Error bars show the standard deviation, indicating the interannual variations of SLA-EMS from 2001 to 2016.

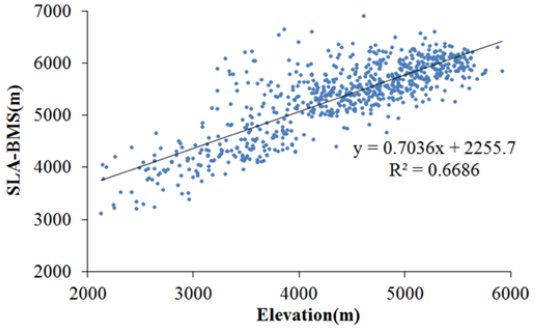

https://doi.org/10.5194/tc-2019-139
Preprint. Discussion started: 18 June 2019

Figure 10. Relationships between SLA-EMS and elevations (30km). The X-axis represents the average elevation of the 30km glacier grids, Y-axis represents the extracted SLA-EMS of the glacier grids.

4.2 Spatiotemporal Variations of SLA-EMS during 2001-2016

Figure 11 illustrates the linear trend (*Slope*) of SLA-EMS and its significance level at the grid scale for the 16 years. On the whole, the SLA-EMS shows a rising trend in HMA, although a large number of glacier grids (40.6%) are characterized by weak trends in SLA-EMS ($-3 < Slope < 3$ m yr^{-1}). The linear trends for SLA-EMS in 75.3% of the grids are increased to different degrees ($0.0 < Slope < 24.5$ m yr^{-1}), and the increase trends in 24.2% of the grids are statistically significant ($P<0.05$). The SLA-EMS increases with the *Slope* greater than 3 m yr^{-1} account for 39.4%. But only 16.1% of the grids are characterized by decrease trends in SLA-EMS ($-13.6 < Slope < 0.0$ m yr^{-1}), and the significant decreased ($P<0.05$) grids even less than 1%. The grids with significant increased SLA-EMS are mainly distributed in Tien Shan, east and central Himalayas, inner Tibet, and the Nyainqentanglha of south and east Tibet. While the weak trends of decrease in SLA-EMS appears in few areas of Karakoram, Pamir, Hindu Kush, and west Himalaya (Figure 11).

https://doi.org/10.5194/tc-2019-139
Preprint. Discussion started: 18 June 2019

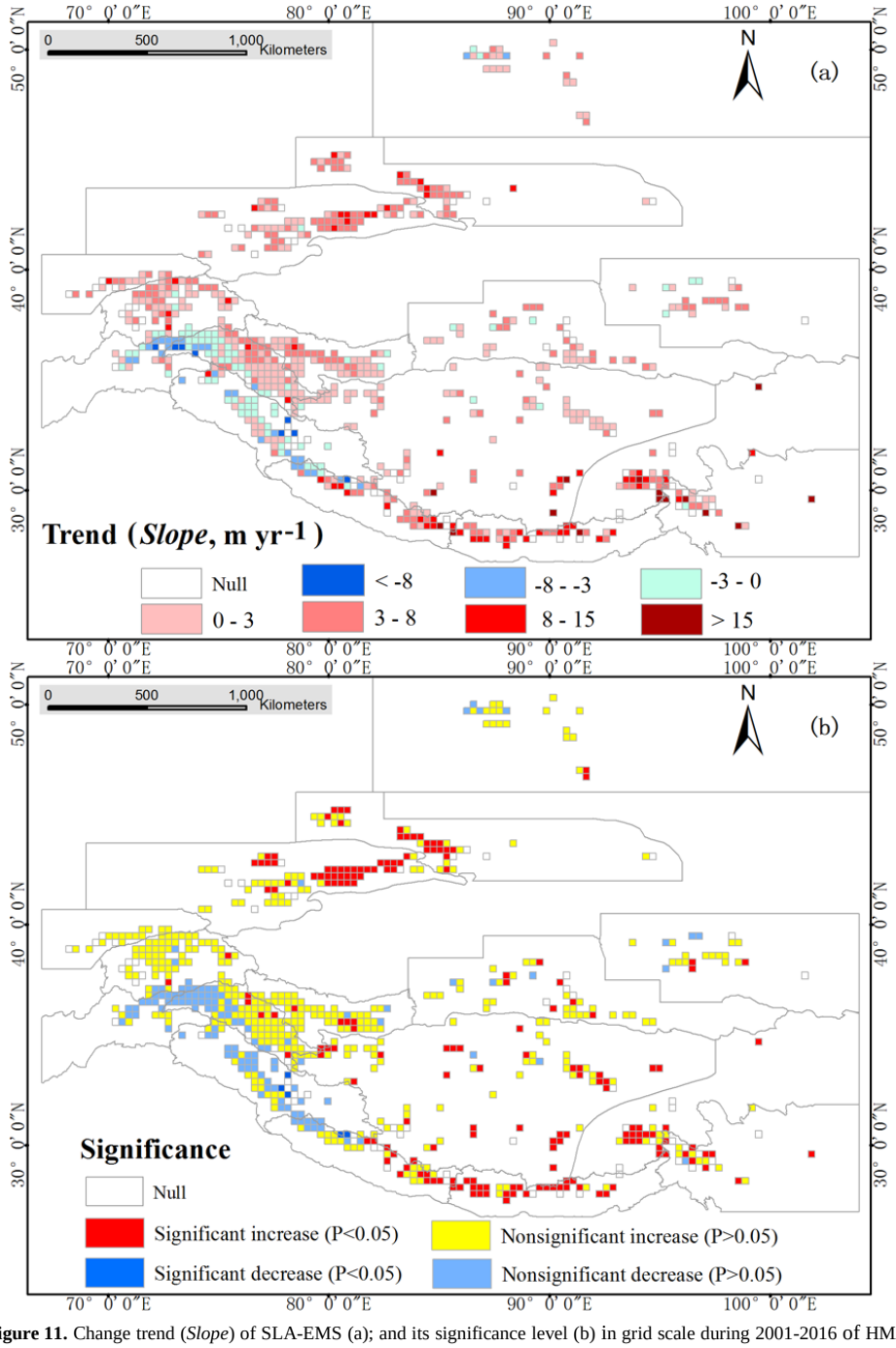

Figure 11. Change trend (*Slope*) of SLA-EMS (a); and its significance level (b) in grid scale during 2001-2016 of HMA. Significant changes indicate its statistical significance at the 5% level.

Figure 12 further present the interannual changes and linear trend (*Slope*) of SLA-EMS for different subregions. Significant increase trends of SLA-EMS during the 16 years are found in Tien Shan, inner Tibet,

https://doi.org/10.5194/tc-2019-139
Preprint. Discussion started: 18 June 2019

The Cryosphere Discussions
Open Access
EGU

south and east Tibet, east Himalaya and Hengduan Shan; especially, in southeastern of HMA (south and east Tibet, east Himalaya and Hengduan Shan), the average SLA-EMS increment is relatively higher (*Slope*≥7.48 m yr^{-1}). While in other regions, the SLA-EMS shows nonsignificant increase or large interannual fluctuation; the large interannual fluctuations of SLA-EMS are mainly located in western HMA (Pamir, Hindu Kush and Hissar Alay). The SLA-EMS in the Karakoram, Pamir, Hindu Kush and west Himalaya show stability or slightly decreasing trend.

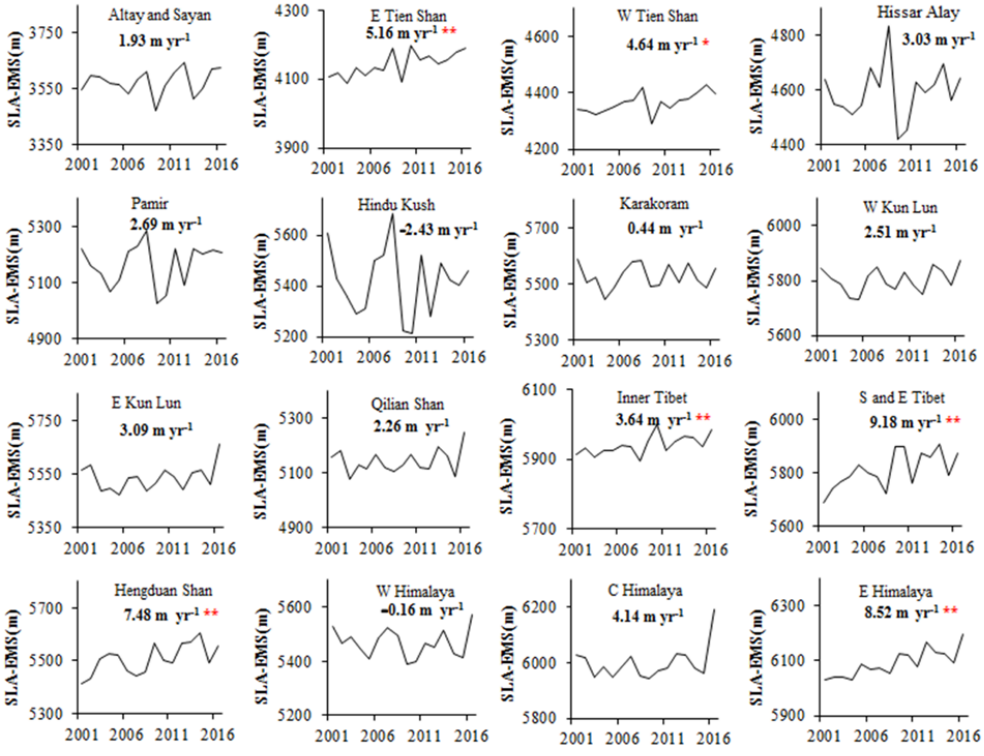

Figure 12. Interannual variation and linear trend (*Slope*) of SLA-EMS for different subregions of HMA from 2001 to 2016. ** and * indicate statistical significance at the 0.01 and 0.05 level, respectively.

4.3. Correlations between SLA-EMS, Temperature and Precipitation

To explore the possible mechanisms for SLA-EMS changes of the HMA, we examined the linkages between the SLA-EMS and two important climate parameters (temperature and precipitation) variations by the correlation analysis. In this study, the in situ climate data from 172 meteorological stations (which are located in the study area) are selected to investigate the relationship between the SLA-EMS, temperature and precipitation from the different subregions. And the temperature and precipitation are divided into two time scales (summer and annual) in the analysis. Change trends of temperature and precipitation in these regions are approximately represented by the stations' average value, although the meteorological stations are scarce and unevenly distributed in some subregions. Table 3 presents the Pearson correlation coefficients between the SLA-EMS, temperature and precipitation for the period of 2001–2016. Although the correlation coefficients between the SLA-EMS and temperature vary in regions, indicating a large spatial heterogeneity, the SLA-EMS in almost all of the regions shows a positive correlation with the temperature, particularly a

https://doi.org/10.5194/tc-2019-139
Preprint. Discussion started: 18 June 2019

significant positive correlation with the summer temperature (the average R= 0.64). While, there is no obvious correlation between SLA-EMS and precipitation. These results suggest that temperature (especially the summer temperature) was the dominant climatic factor affecting the interannual variations of SLA-EMS in the study area, and the variation trend and high fluctuation of SLA-EMS in the HMA (Figure 12) is mostly due to the variability of temperature. The rising temperature in the snowmelt period can increase snow melting and decrease snowfall, both of which can lead to a higher SLA-EMS. If the global warming trend continues, the increase of the SLA-EMS caused by the high-positive correlation with temperature may result in significant changes in water resources and river flows in the HMA. This will exert effects on the ecosystem, irrigation-dependent agriculture, and domestic water in the densely populated downstream areas.

Table 3. Pearson correlation coefficients between the SLA-EMS, temperature, and precipitation in different subregions for the period of 2001–2016.

Regions	Summer temperature	Annual temperature	Summer precipitation	Annual precipitation
S and E Tibet	0.69 **	0.72 **	0.42	0.40
Hengduan Shan	0.34	0.34	0.29	-0.01
Qilian Shan	0.72 **	0.60 *	0.19	0.03
Inner Tibet	0.32	0.13	-0.26	-0.23
E Tien Shan	0.60 *	0.22	-0.01	0.08
W Tien Shan	0.76 **	0.29	0.00	-0.16
E Himalaya	0.67 **	0.38	-0.14	-0.21
E Kun Lun	0.64 **	0.47	-0.09	-0.06
C Himalaya	0.58 *	0.53 *	0.31	-0.23
Pamir	0.75 **	0.37	0.02	-0.02
W Himalaya	0.83 **	0.55 *	0.01	-0.01
Altay and Sayan	0.66 **	0.12	0.28	0.02
Hissar Alay	0.83 **	0.11	N.A.	N.A.
Hindu Kush	0.63 **	0.26	N.A.	N.A.
W KunLun	N.A.	N.A.	N.A.	N.A.
Karakoram	N.A.	N.A.	N.A.	N.A.

Note: ** and * indicate statistical significance at the 0.01 and 0.05 level, respectively. The regions without meteorological stations (or missing data) are represented by “N.A.” (meaning “not available”).

5. Discussion

Satellite remote sensing data has been used to monitor regional snowline altitude for a long time, and visual interpretation of Landsat MSS, TM and ETM+ (and so on) images observed in the end of summer is the common method for investigating the SLA-EMS changes in a local areas (McFadden et al., 2011; Pandey et al., 2013; Rabatel et al., 2012; Tawde et al., 2016; Zhang and Kang, 2017). Since the 2000s, the MODIS snow cover products provide an excellent opportunity to study the snow cover for global or large-scale areas, and they have been used to investigate the spatiotemporal changes of the seasonal or transient snowline altitude (Krajčí et al., 2016; Krajčí et al., 2014; Parajka et al., 2010; Spiess et al., 2016; Tang et al., 2014; Verbyla et al., 2017). However, there is still little suitable method to assessing large-scale SLA-EMS changes using

https://doi.org/10.5194/tc-2019-139
Preprint. Discussion started: 18 June 2019

MODIS snow cover product. Therefore, a methodology of SLA-EMS determination from cloud-removed MODIS snow cover products is developed in this study. The highlights of this methodology can be summarized as follows: (1) the cloud cover in MODIS snow cover products were effectively removed; (2) in order to accurately estimate the perennial snow cover, the MODIS SCD threshold was calibrated using both the glaciers annual mass balance observations and Landsat images; (3) dividing glacier grids, and determination altitude value of SLA-EMS on a grid-by-grid basis using the area-elevation distribution curve and the perennial snow cover area. This study can also be intended as a precedent toward using MODIS snow cover products to assess SLA-EMS at the large-scale areas for better understanding of water resources and climatology of cold region. However, we cannot ignore the limitations of using the coarse resolution dataset (500m); the MODIS dataset is not suitable for the extraction of SLA-EMS in small-scale area, and this is also why the glacier grids are divided as big to 30km in the study.

Although earlier studies have shown that the snowline identified by satellite images at the end of the glaciological year can be used as an indicator of the glacier annual mass balance (Braithwaite, 1984; Rabatel et al., 2005, 2008, 2012; Xie et al., 1996), the glacier mass balance is presently estimated by three main methods. Glaciological method (also known as field estimate) is one of the most commonly used method, where glacier mass balance is estimated using in situ field studies. But, due to mountainous terrain and logistic reasons, this method is limited to a few glaciers. The second method is the local remote sensing analysis (geodetic method using DEM differencing). Geodetic method provided mass balance estimates only for areas smaller than a few thousand square kilometres (Pieczonka and Bolch, 2015; Rankl and Braun, 2016; Shangguan et al., 2015) and for varying periods, and has demonstrated that these sub-regional measurements are not representative at the larger scale (Gardner et al., 2013). The third method is large-scale satellite measurements, such as laser altimetry (ICESat). However, ICESat-1 laser altimeter operated only from 2003 to 2009, and had a sparse spatial sampling leading to potential large bias (Treichler and Kääb, 2016). Therefore, it is still difficult to achieve continuous spatial-temporal monitoring of the glacier mass balance for a large scale area. In this work, we find that there is a good linear regression relationship between the grid (30km) SLA-EMS and annual mass balance of glaciers in the HMA (Figure 5 and Table 1). The SLA-EMS is negatively related with the glaciers annual mass balance (the average correlation coefficients is -0.66). These demonstrate that the MODIS extracted grid SLA-EMS can be a good indicator of large-scale glaciers annual mass balance. The proposed SLA-EMS determination method and SLA-EMS datasets in this research will have good potential in reconstruction or extending the glacier annual mass balance time series at large-scale area such as the HMA. However, the quantitative relationship between SLA-EMS and glacier annual mass balance needs to be further studied in the future work using more abundant glacier annual mass balance data, for example using time series of DEMs derived from ASTER optical satellite stereo-images (Brun et al., 2017).

The spatial distribution pattern of SLA-EMS in the HMA is mainly affected by two factors: latitude and topographic altitude (Firgure 8 and 10). And the spatial pattern of SLA-EMS (Firgure 8) in this study is very in keeping with the spatial distributions of the ELA of the monitoring glaciers in High Asia (Ye et al., 2016). The latitudinal distribution pattern of SLA-EMS manifest as the SLA-EMS gradually decreasing from south to north, that is Himalayas > inner Tibet > KunLun > Tien Shan > Altay and Sayan (Firgure 8). The differences in solar radiation and temperature caused by latitude could be the main reason for latitudinal pattern of SLA-EMS. The significant positive correlation between SLA-EMS and elevation (Firgure 10), that is, the topographic altitude controlled spatial pattern of the SLA-EMS could be ascribed to the mass elevation

https://doi.org/10.5194/tc-2019-139
Preprint. Discussion started: 18 June 2019

effect, which is essentially the result of the thermodynamic effect of mountain masses (Han et al., 2018; ZHANG et al., 2016), and virtually leading to higher temperature in the interior than in the outside of mountain masses at same elevation and on similar latitudes, and has been recognized as a significant contributor to the vertical distribution of mountain snowline and timberline (Han et al., 2012; Han et al., 2011).

Under the context of global warming, the cryosphere (snow cover, glaciers, glacial lakes and permafrost) of the HMA has been changing rapidly (Brun et al., 2017; Cheng and Wu, 2007; Rittger et al., 2016; Yao et al., 2012; Zhang et al., 2015). Like many glaciers worldwide, the glaciers in HMA have generally been losing mass over the past decades, but a subset of glaciers in the region have been stable or even slight growing. This peculiar behavior, first observed over the Karakoram and often named the "Karakoram anomaly" (Hewitt, 2005), has been demonstrated in the Karakoram and Pamir mountains in northwest HMA (BOLCH, et al., 2012; Gardelle et al., 2012). Recent work shows the "anomaly" of glaciers mass balances even toward the northeast of the Karakoram, in the west KunLun region (Brun et al., 2017; Lin et al., 2017). In this work, we find the SLA-EMS in HMA generally shows a rising trend in the 16 years (Figure 11 and 12), and the significant increase trends of SLA-EMS are mainly located in east Tien Shan (5.16 m yr^{-1}), west Tien Shan (4.64 m yr^{-1}), Inner Tibet (3.64 m yr^{-1}), south and east Tibet (9.18 m yr^{-1}), east Himalaya (8.52 m yr^{-1}), and Hengduan Shan (7.48m yr^{-1}). These rising trends of SLA-EMS may indicate decreases in glacial annual mass balance in the 16 years. Under the background of the generally losing glaciers mass in these areas (i.e. average annual mass balance is already negative), if the SLA-EMS continues to rise as a result of global warming, it will accelerate the negative mass balances of the glaciers. While, in the glacier mass balance anomaly areas, such as Karakoram, Pamir, Hindu Kush and west KunLun, the SLA-EMS shows no obvious trend during the examined period although a strong interannual variability is discovered.

It is true that the meteorological stations used in the correlation analysis of this study are heterogeneous and mostly located in the valley, which may not accurate represent the temperature and precipitation conditions at higher altitudes where the glaciers and perennial snow cover frequently presents. While, strong linkage between the SLA-EMS and temperature is found. That is, Temperature (especially the summer temperature) was the dominant climatic factor affecting the changes of SLA-EMS in HMA (Table 3). However, the effect of climate change on SLA-EMS is very complex. First, the other climate factors such as intensity of solar radiation, vapor pressure, wind velocity, and their synergistic effect also give rise to SLA-EMS variation, which should not be ignored. Second, climate changes and their effect on snow cover vary with geographical environment, like the regions of "Karakoram anomaly". Furthermore, the period of 16 years, is a long time considering available MODIS information, while is not sufficient for statements about climate change. Most of the trends for SLA-EMS change are not reached at the statistical significant level. A longer time series of data needs to be examined in further studies to obtain some more definitive conclusions about temporal trends of SLA-EMS and the relationship with climate change.

6. Conclusions

This study presents a large-scale SLA-EMS monitoring method based on the cloud-removed daily MODIS FSC data. In this method, the extent of HMA is divided into 744 glacier grids (30km); the MODIS SCD threshold for estimating perennial snow cover and SLA-EMS is deliberately calibrated using glaciers mass

https://doi.org/10.5194/tc-2019-139
Preprint. Discussion started: 18 June 2019

balance observations and Landsat images; and the altitude value of the SLA-EMS for these glacier grids is extracted using the area-elevation distribution curve (from DEM) and the perennial snow cover area. We examine large-scale spatial patterns of the SLA-EMS across HMA and identify trends over the past 16 years, and also explore the possible linkage between SLA-EMS and temperature and precipitation. The main findings are summarized as the follows:

(1) There are good linear regression relationships (the average R = -0.66) between the grid (30km) SLA-EMS and glaciers annual mass balance over the HMA. This implies that the SLA-EMS monitoring method could help reconstruction or extending the glacier annual mass balance time series at large-scale area. However, the quantitative relationships between SLA-EMS and glaciers annual mass balance are spatially complex and will require further spatially resolved assessments and using more abundant glacier annual mass balance data.

(2) The spatial pattern of SLA-EMS across HMA is mainly affected by two factors: latitude and topographic altitude. The latitudinal pattern of SLA-EMS manifest as the gradually decreasing from south to north, that is Himalayas > inner Tibet > KunLun > Tien Shan > Altay and Sayan. Due to the mass elevation effect, the SLA-EMS decreases from the high altitude region of Himalayas and inner Tibet to surrounding low mountainous area.

(3) The SLA-EMS of HMA generally shows a rising trend in the recent years (2001-2016). In total, 75.3% (24.2% with a significant increase) and 16.1% (less than 1% with a significant decrease) of the glacier grids in HMA show increasing and decreasing trends in SLA-EMS, respectively. The SLA-EMS significant increases in Tien Shan, Inner Tibet, south and east Tibet, east Himalaya and Hengduan Shan; while there are no obvious trends in the Karakoram, Pamir, Hindu Kush, west KunLun and west Himalaya.

(4) The SLA-EMS over the HMA shows a positive correlation with the temperature, particularly a significant positive correlation with the summer temperature (R= 0.64), while no obvious correlation with precipitation. Temperature (especially the summer temperature) was the dominant climatic factor affecting the variations of SLA-EMS over the HMA. If the global warming continues, the rising of the SLA-EMS may accelerate the negative mass balances of the most glaciers over the HMA, lead to change the flow regimes and water availability, thus impacting ecosystem, agriculture and water resources in the densely populated downstream areas.

Acknowledgments: Many thanks to Etienne Berthier (the Editor) for insightful comments which has improved this manuscript. This study was financially supported by the National Natural Science Foundation of China (Grant No. 41871058, 41501070), Natural Science Foundation of Hunan Province, China (Grant No. 2018JJ3154), and the National Natural Science Foundation of China (Grant No. 41771075, 41701061).

Author Contributions: Zhiguang Tang conceived and designed the study, and wrote the paper. Zhiguang Tang and Xiaoru Wang contributed to the development of the methodology and performed the experiments. Xiaoru Wang analyzed the data. Jian Wang, Xin Wang and Junfeng Wei contributed to discussions and revisions.

Conflicts of Interest: The authors declare that they have no conflict of interest.

https://doi.org/10.5194/tc-2019-139
Preprint. Discussion started: 18 June 2019

References

Barnett, T. P., Adam, J. C., and Lettenmaier, D. P.: Potential impacts of a warming climate on water availability in snow-dominated regions. Nature, 438, 303-309, 2005.

Bolch, T., Kulkarni, A. V., Kääb, A., Huggel, C., Paul, F., Cogley, J. G., Frey, H., Kargel, J. S., Fujita, K., Scheel, M., Bajracharya S., and Stoffel, M.: The state and fate of Himalayan glaciers. Science, 336, 310-314, 2012.

Braithwaite R. J.: Can the mass balance of a glacier be estimated from its equilibrium-line altitude?. J. Glaciol., 30, 364-368, 1984.

Brun, F., Berthier, E., Wagnon, P., Kääb, A., and Treichler, D.: A spatially resolved estimate of High Mountain Asia glacier mass balances from 2000 to 2016. Nat. Geosci., 10, 668-675, 2017.

Chen, Y., Li, Z., Fang G., and Deng H.: Impact of climate change on water resources in the Tianshan Mountians, Central Asia. Acta Geographica Sinica, 72, 18-26, 2017 (in Chinese).

Cheng, G., and Wu, T.: Responses of permafrost to climate change and their environmental significance, Qinghai-Tibet Plateau. J. Geophys. Res., 112-121, 2007.

Duethmann, D., Bolch, T., Farinotti, D., Kriegel, D., Vorogushyn, S., Merz, B., Pieczonka, T., Jiang, T., Su, B., and Güntner, A.: Attribution of streamflow trends in snow and glacier melt - dominated catchments of the Tarim River, Central Asia. Water Resour. Res., 51, 4727-4750, 2015.

Dwyer, M. J., and Schmidt, G.: The MODIS reprojection tool, in: Earth Science Satellite Remote Sensing, edited by: Qu, J. J., Gao, W., Kafatos, M., and Salomonson, V.V., Springer, Berlin, Heidelberg, Germany, 162-177, 2006.

Flint, R. F.: Glacial and Quaternary geology. New York: John Wiley Press, 1971.

Gafurov, A., and Bárdossy, A.: Cloud removal methodology from MODIS snow cover product. Hydrol. Earth Syst. Sci., 13, 1361-1373, 2009.

Gardelle, J., Berthier, E., and Arnaud, Y.: Slight mass gain of Karakoram glaciers in the early twenty-first century. Nat. Geosci., 5, 322-325, 2012.

Gardner, A. S., Moholdt, G., Cogley, J. G., Wouters, B., Arendt, A. A., Wahr, J., Berthier, E., Hock, R., Pfeffer, W. T., Kaser, G., Ligtenberg, S. R., Bolch, T., Sharp, M. J., Hagen, J. O., van den Broeke, M. R., Paul, F.: A reconciled estimate of glacier contributions to sea level rise: 2003 to 2009. Science, 340, 852-857, 2013.

Hall, D. K., and Riggs, G. A.: Accuracy assessment of the MODIS snow products. Hydrol. Process., 21, 1534-1547, 2007.

Hall, D. K., Riggs, G. A., and Salomonson, V. V.: Development of methods for mapping global snow cover using moderate resolution imaging spectroradiometer data. Remote Sens. Environ., 54, 127-140, 1995.

Han, F., Yao, Y., Dai, S., Wang, C., Sun, R., Juan, X., and Zhang, B.: Mass elevation effect and its forcing on timberline altitude. J. Geogr. Sci., 22, 609-616, 2012.

Han, F., Zhang, B., Yao, Y., Zhu, Y., and Pang, Y.: Mass elevation effect and its contribution to the altitude of snowline in the Tibetan Plateau and surrounding areas. Arct. Antarct. Alp. Res., 43, 207-212, 2011.

Han, F., Zhang, B.P., Zhao, F., Guo, B., and Liang, T.: Estimation of mass elevation effect and its annual variation based on MODIS and NECP data in the Tibetan Plateau. Journal of Mountain Science, 15, 1510-1519, 2018.

https://doi.org/10.5194/tc-2019-139
Preprint. Discussion started: 18 June 2019

Hewitt, K.: The Karakoram anomaly? Glacier expansion and the 'elevation effect,' Karakoram Himalaya. Mt. Res. Dev., 25, 332-340, 2005.

Holzer, T., Baumgartner, M. F., and Apfl, G.: Monitoring Swiss alpine snow cover variations using digital NOAA-AVHRR data. In IEEE International Geoscience and Remote Sensing Symposium, 1765-1767, 1995.

Hu, Z., Zhang, C., Hu, Q., and Tian, H.: Temperature changes in central Asia from 1979 to 2011 based on multiple datasets. J. Climate, 27, 1143-1167, 2013.

Immerzeel, W. W., van Beek, L. P., and Bierkens, M. F.: Climate change will affect the Asian water towers. Science, 328, 1382-1385, 2010.

Kaur, R., Kulkarni, A. V., and Chaudhary, B.: Using RESOURCESAT-1 data for determination of snow cover and snowline altitude, Baspa Basin, India. Ann. Glaciol., 51, 9-13, 2010.

Klein, A., Barnett, A., and Lee, S.: Evaluation of MODIS snow cover products in the Upper Rio Grande River Basin. In, EGS - AGU - EUG Joint Assembly, 5, 2003.

Krajčí, P., Holko, L., Perdigão, R. A., and Parajka, J.: Estimation of regional snowline elevation (RSLE) from MODIS images for seasonally snow covered mountain basins. J. Hydrol., 519, 1769-1778, 2014.

Krajčí, P., Holko, L., and Parajka, J.: Variability of snow line elevation, snow cover area and depletion in the main Slovak basins in winters 2001–2014. J. Hydrol. Hydromech., 64, 12-22, 2016.

Lei, L., Zeng, Z., and Zhang, B.: Method for detecting snow lines from MODIS data and assessment of changes in the Nianqingtanglha mountains of the Tibet plateau. IEEE J-STARS., 5, 769-776, 2012.

Lin, H., Li, G., Lan, C., Hooper, A., and Ye, Q.: A decreasing glacier mass balance gradient from the edge of the Upper Tarim Basin to the Karakoram during 2000–2014. Scientific Reports, 7, 2017.

Lutz, A. F., Immerzeel, W. W., Shrestha, A. B., and Bierkens, M. F. P.: Consistent increase in High Asia's runoff due to increasing glacier melt and precipitation. Nat. Clim. Change, 4, 587–592, 2014.

Martinec, J., Rango, A., and Roberts, R.: SRM snowmelt runoff model user's manual. Department of Geography, Univ. of Berne, Berne, Switzerland. 2008.

McFadden, E., Ramage, J., and Rodbell, D.: Landsat TM and ETM+ derived snowline altitudes in the Cordillera Huayhuash and Cordillera Raura, Peru, 1986–2005. The Cryosphere, 5, 419-430, 2011.

Pandey, P., Kulkarni, A. V., and Venkataraman, G.: Remote sensing study of snowline altitude at the end of melting season, Chandra-Bhaga basin, Himachal Pradesh, 1980–2007. Geocarto Int., 28, 311-322, 2013.

Parajka, J., Pepe, M., Rampini, A., Rossi, S., and Blöschl, G.: A regional snow-line method for estimating snow cover from MODIS during cloud cover. J. Hydrol., 381, 203-212, 2010.

Parker, S. P.: Dictionary of Earth Science. McGraw-Hill Higher Education, New York, USA, 1997.

Pieczonka, T., and Bolch, T.: Region-wide glacier mass budgets and area changes for the Central Tien Shan between ~ 1975 and 1999 using Hexagon KH-9 imagery. Global Planet. Change, 128, 1-13, 2015.

Qiu, J.: China: The third pole. Nature, 454, 393-396, 2008.

Rabatel, A., Dedieu, J. P., and Vincent, C.: Using remote-sensing data to determine equilibrium-line altitude and mass-balance time series: validation on three French glaciers, 1994-2002. J. Glaciol., 51, 539-546, 2005.

Rabatel, A., Dedieu, J. P., Thibert, E., Letréguilly, A., and Vincent, C.: 25 years (1981–2005) of equilibrium-line altitude and mass-balance reconstruction on Glacier Blanc, French Alps, using remote-sensing methods and meteorological data. J. Glaciol., 54, 307-314, 2008.

https://doi.org/10.5194/tc-2019-139
Preprint. Discussion started: 18 June 2019

562 Rabatel, A., Bermejo, A., Loarte, E., Soruco, A., Gomez, J., Leonardini, G., Vincent, C., and Sicart, J. E.: Can
563 the snowline be used as an indicator of the equilibrium line and mass balance for glaciers in the outer
564 tropics? J. Glaciol., 58, 1027-1036, 2012.
565 Rankl, M., and Braun, M. H.: Glacier elevation and mass changes over the central Karakoram region
566 estimated from Tan DEM-X and SRTM/X-SAR digital elevation models. Ann. Glaciol., 51, 273-281,
567 2016.
568 Riggs, G., Hall, D., and Salomonson, V.: MODIS snow products user guide to collection 5. 2006. Available
569 online: https://modis-snow-ice.gsfc.nasa.gov/ (accessed on 10 May 2014).
570 Rittger, K., Brodzik, M. J., Painter, T. H., Racoviteanu, A., Armstrong, R., and Dozier, J.: Trends in annual
571 minimum exposed snow and ice cover in High Mountain Asia from MODIS. In EGU General Assembly
572 Conference,18, 2016.
573 Salomonson, V., and Appel, I.: Estimating fractional snow cover from MODIS using the normalized
574 difference snow index. Remote Sens. Environ., 89, 351-360, 2004.
575 Seidel, K., Ehrler, C., Martinec, J., and Turpin, O.: Derivation of statistical snowline from high resolution
576 snow cover mapping. In EARSeL Workshop: Remote Sensing of Land Ice and Snow, 31-36, 1997.
577 Shangguan, D. H., Bolch, T., Ding, Y. J., Kröhnert, M., Pieczonka, T., Wetzel, H. U., and Liu, S. Y.: Mass
578 changes of Southern and Northern Inylchek Glacier, Central Tian Shan, Kyrgyzstan, during ~ 1975 and
579 2007 derived from remote sensing data. The Cryosphere, 9, 703-717, 2015.
580 Spiess, M., Huintjes, E., and Schneider, C.: Comparison of modelled- and remote sensing- derived daily snow
581 line altitudes at Ulugh Muztagh, northern Tibetan Plateau. Journal of Mountain Science, 13, 593-613,
582 2016.
583 Tang, Z., Wang, J., Li, H., and Yan, L.: Spatiotemporal changes of snow cover over the Tibetan plateau based
584 on cloud-removed moderate resolution imaging spectroradiometer fractional snow cover product from
585 2001 to 2011. J. Appl. Remote Sens., 7, 073582, 2013.
586 Tang, Z., Wang, J., Li, H., Liang, J., Li, C., and Wang, X.: Extraction and assessment of snowline altitude
587 over the Tibetan plateau using MODIS fractional snow cover data (2001 to 2013). J. Appl. Remote Sens.,
588 8, 084689, 2014.
589 Tang, Z., Wang, X., Wang, J., Wang, X., Li, H., and Jiang, Z.: Spatiotemporal variation of snow cover in
590 Tianshan mountains, Central Asia, based on cloud-free MODIS fractional snow cover product,
591 2001–2015. Remote Sensing, 9, 1045, 2017.
592 Tawde, S., Kulkarni, A. V., and Govindasamy, B.: Estimation of glacier mass balance on a basin scale:an
593 approach based on satellite-derived snowlines and a temperature index model. Current Science, 111,
594 1977-1989, 2016.
595 Treichler, D., and Kääb, A.: ICES at laser altimetry over small mountain glaciers. The Cryosphere, 10,
596 2129-2146, 2016.
597 Turpin, O. C., Ferguson, R. I., and Clark, C. D.: Remote sensing of snowline rise as an aid to testing and
598 calibrating a glacier runoff model. Phys. Chem. Earth, 22, 279-283, 1997.
599 Verbyla, D., Hegel, T., Nolin, A., Kerk, M. V. D., Kurkowski, T., and Prugh, L.: Remote sensing of
600 2000–2016 alpine spring snowline elevation in Dall sheep mountain ranges of Alaska and western
601 Canada. Remote Sensing, 9, 1157, 2017.

https://doi.org/10.5194/tc-2019-139
Preprint. Discussion started: 18 June 2019

Wang, X., and Xie, H.: New methods for studying the spatiotemporal variation of snow cover based on combination products of MODIS Terra and Aqua. J. Hydrol., 371, 192-200, 2009.

WGMS: Glacier mass balance bulletin, No. 1-12. World glacier monitoring service (WGMS): Zurich, Switzerland, 1991-2013. Available online: https://wgms.ch/literature_published_by_wgms/.

WGMS: Fluctuations of glaciers database. World glacier monitoring service (WGMS): Zurich, Switzerland, 2017. Available online: https://wgms.ch/data_databaseversions/ (accessed on 21 May 2017).

Xie, H., Liang, T., and Wang, X.: Development and assessment of combined Terra and Aqua snow cover products in Colorado Plateau, USA and northern Xinjiang, China. J. Appl. Remote Sens., 3, 033559, 2009.

Xie, Z., Ding L., Liu C., and Liu, S.: Mass balance at the steady state equilibrium line altitude and its application. Journal of Glaciolgy and Geocryology, 18, 1-9, 1996 (in Chinese).

Yao, T., Thompson, L. G., Mosbrugger, V., Zhang, F., Ma, Y., Luo, T., Xu, B., Yang, X., Joswiak, D. R., and Wang, W.: Third pole environment (TPE). Environmental Development, 3, 52-64, 2012.

Ye, W., Wang, F., Li, Z., Zhang, H., Xu, C., and Hu, A.: Temporal and spatial distributions of the equilibrium line altitudes of the monitoring glaciers in High Asia. Journal of Glaciology and Geocryology, 38, 1459-1469, 2016 (in Chinese).

Zappa, M.: Objective quantitative spatial verification of distributed snow cover simulations—an experiment for the whole of Switzerland/Vérification quantitative spatiale objective de simulations distribuées de la couche de neige—une étude pour l'ensemble de la Suisse. Hydrolog. Sci. J., 53, 179-191, 2008.

Zhang, B., and Yao Y.: Implications of mass elevation effect for the altitudinal patterns of global ecology. J. Geogr. Sci., 26, 871-877, 2016a.

Zhang, G., Yao, T., Xie, H., Wang, W., and Wei, Y.: An inventory of glacial lakes in the Third Pole region and their changes in response to global warming. Global. Planet. Change, 131, 148-157, 2015.

Zhang, Q., and Kang, S.: Glacier snowline altitude variations in the Pamirs, Tajikistan, 1998-2013: insights from remote sensing images. Remote Sens. Lett., 8, 1221-1230, 2017.

Zhang, Y., Cao, T., Kan, X., Wang, J., and Tian, W.: Spatial and temporal variation analysis of snow cover using MODIS over Qinghai-Tibetan Plateau during 2003–2014. J. Indian Soc. Remote., 45, 1-11, 2016b.